Kinetic theory of flux-driven ripening

A. M. Gusak* and K. N. Tu
Department of Materials Science and Engineering, UCLA, Los Angeles, California 90095-1595
(Received 24 September 2001; revised manuscript received 26 February 2002; published 4 September 2002)

The classic Lifshitz-Slezov-Wagner theory of ripening assumes that within a closed system, the total volume of the phase undergoing ripening remains constant while the total surface area of the phase decreases. We present here the ripening behavior in an open system in which the total surface area of the phase undergoing ripening remains constant while the total volume of the phase is growing. We define the latter growth to be flux-driven ripening. We compare these two types of ripening, one within a closed system and the other within an open system, in terms of the particles' size distribution function, the scaling behavior of the distribution, and the rate of growth of the mean particle size.

DOI: 10.1103/PhysRevB.66.115403 PACS number(s): 68.08.Bc, 81.10.Fq, 64.70.Dv

I. INTRODUCTION

In first-order phase transformations, ripening typically occurs after nucleation and growth. The classic Lifshitz-Slezov-Wagner (LSW) theory of ripening assumes that this occurs in a closed system.[1–3] In such a system, while the total volume of the phase undergoing ripening is very small, it remains constant. Because the volume or mass is preserved, this is a conservative process. The driving force of LSW ripening is the reduction of surface area or surface energy of the phase. Thus, the total surface area of the phase decreases during ripening. Recently, in studies of the interfacial reaction between molten solder and metal, ripening of the scallop-type intermetallic compound phase at the interface was found to be accompanied by growth; i.e., ripening and growth occur simultaneously. Since the volume of the compound phase increases with time, this type of ripening is considered nonconservative. The driving force is the gain in free energy of the compound phase growth. What is very surprising in this process is that the total surface area of the compound phase can be treated as constant during its growth provided that we assume the scallops are hemispherical particles. Scallop-type growth is widely recognized in solder reactions between eutectic SnPb and Cu.[4–9] It also occurs between Pb-free solders (such as eutectic SnAg) and Cu,[10–13] and also between pure Sn and Cu.[14–17] In 1996, Kim and Tu analyzed the kinetics of the ripening of scallop-type growth.[12] However, in their analysis, two key aspects were ignored. The first aspect ignored was the crucial constraint of constant surface area during ripening. The second aspect not considered was the particle size distribution function.

In this paper, we present a kinetic theory of ripening which features constancy in surface accompanied by volume growth. We define this as flux-driven ripening (FDR). The particle size distribution function of the theory has been derived. The time-dependent behavior of the mean size particle and its growth rate are presented. We also present an alternative derivation of the classical LSW particle size distribution function. Hence, we make a comparison between these two kinds of size distribution functions; one corresponds to ripening with a constant volume but decreasing surface, while the other corresponds to a constant surface but increasing volume. The different predictions as derived from these two size distribution functions are also herein discussed.

II. BASIC ASSUMPTIONS IN RIPENING UNDER CONSTANT SURFACE AND GROWING VOLUME

A brief review of the reactions between molten eutectic SnPb and Cu, as well as between molten Sn and Cu, is presented here as examples to delineate the basic assumptions needed for theoretical development. Eutectic SnPb solder has a melting point of 183 °C, so the solder reaction typically occurs at 200 °C, lasting anywhere from a few seconds to several minutes. In the case of pure Sn on Cu, since Sn melts at 237 °C, the reaction temperature is typically around 250 °C. In these reactions, Cu_6Sn_5 and Cu_3Sn intermetallic compounds (IMC's) are formed at the interfaces. The Cu_6Sn_5 is the dominant growth phase and has scallop-type morphology. The size of the scallops can grow to several microns in diameter after a few minutes of reaction at 200 °C between eutectic SnPb and Cu. On a given area of the interface, the scallops were found to grow bigger but fewer with time. Assuming a hemispherical shape, the radius of scallops was found to obey an approximately $t^{1/3}$ dependence of growth, t being time. The number of scallops decreases at an approximately $t^{-2/3}$ dependence.[12,16] The activation energy of the growth, measured from the growth rates occurring from 200 to 240 °C during the reaction between eutectic SnPb and Cu, is about 0.2–0.3 eV/atom.[12] On the other hand, the Cu_3Sn is a thin layer and its growth is very slow. In the solder reaction at 200 °C for a few minutes, the formation of Cu_3Sn is hardly detectable by scanning electron microscopy.

To simplify the theoretical analysis, we make the following assumptions. (a) The presence of Cu_3Sn and Pb in the reaction is ignored for convenience in the analysis. Figure 1(a) shows a schematic diagram of the cross section of an array of hemispherical Cu_6Sn_5 scallops grown on Cu, represented by the solid curves. (b) There is a liquid channel between two scallops, the depth of which reaches the Cu surface. The width of the channel "δ" is assumed to be small as compared to the radius of scallops. We also assume that the morphology of scallops and channels is thermodynamically stable in the presence of molten solder. This assumption is supported by the observation that molten eutectic SnPb solder wets the grain boundaries of Cu_6Sn_5 instantaneously.[18–20] The channels serve as rapid diffusion paths for Cu to go into the molten solder to grow the scallops. Figure 1(b) is a scanning electron microscopic image of

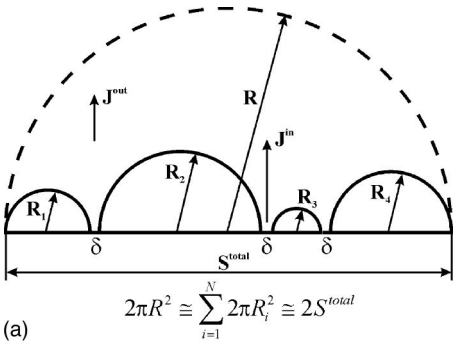

$$2\pi R^2 \cong \sum_{i=1}^{N} 2\pi R_i^2 \cong 2S^{total}$$

(a)

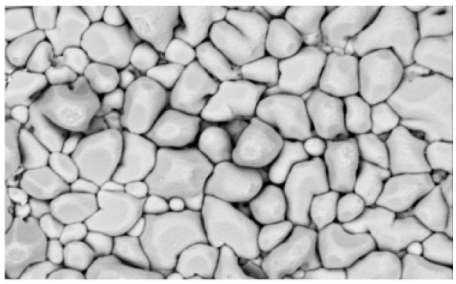

(b)

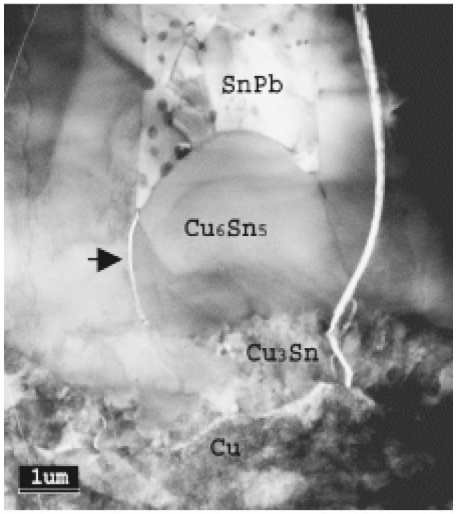

(c)

FIG. 1. Scalloplike morphology of Cu_6Sn_5 during wetting reactions between molten eutectic SnPb solder and Cu. Schematic diagram of the cross section of an array of scallops on Cu. J_{in} is an influx from the substrate into the melt via channels (serving for the growth of scallops), J_{out} is an outflux of copper which was not used for building up the intermetallic compound. For small solder bumps this outflux quickly tends to zero after their saturation. (b) Scalloplike morphology of Cu_6Sn_5 during wetting reactions between molten eutectic SnPb solder and Cu. Scanning electron microscope (SEM) image of the top view of Cu_6Sn_5 scallops after 1 min reflow at 200 °C. SEM images of the cross-sectional view of Cu_6Sn_5 scallops have been published in Ref. 4–9. (c) Scalloplike morphology of Cu_6Sn_5 during wetting reactions between molten eutectic SnPb solder and Cu. Cross-sectional transmission electron microscope (TEM) image of Cu_6Sn_5 scallops after 10 min reflow at 200 °C and channels (indicated by an arrow).

the top view of a group of Cu_6Sn_5 scallops after the solder has been etched away. Although the scallops are separated by channels, they remain in close contact with each other. Figure 1(c) is a cross-sectional transmission electron microscopic image of Cu_6Sn_5 scallops, channels, and a thin layer of Cu_3Sn on Cu. The channel, as indicated by an arrow, has a width less than 50 nm. (c) The shape of the scallops is represented by a hemisphere. On a given interfacial area of "S^{total}" between the scallops and the Cu, the total surface area between all hemispherical scallops and molten solder is just twice S^{total}. In Fig. 1(a), if we represent the cross section of a large hemispherical scallop by the broken half circle, its surface is $2S^{total}$, the same as the sum of the surfaces of the smaller scallops represented by the solid curves. We note that Fig. 1(a) is a two-dimensional diagram representing a three-dimensional growth. Hence, while the growth increases the total volume, it does not change the total surface area of the scallops. Here, we ignore the cross-sectional area of the channels on the interface since δ is very small. (d) All the in-flux of Cu from the Cu substrate is consumed by the growth of the scallops. Furthermore, we assume that the interfacial diffusion of Cu along the scallop/Cu interface is not the rate-limiting factor of the scallop growth. This assumption is supported by the fact that the activation energy of scallop growth is extremely low. (e) We assume the out-flux of Cu from the ripening zone into the bulk of the molten solder to be negligible. This assumption is valid when the solubility of Cu in the molten solder is very low. More discussion and justification of the above assumptions on in-flux and out-flux of Cu are given in Appendix A.

Since the growth of a scallop must occur at the expense of its neighbors, it is a ripening process. In this ripening process, there are two important constraints. The first constraint is that the interface of the reaction is constant. The second is a conservation of mass, in which all the in-flux of Cu is consumed by scallop growth. We also note that this flux-driven ripening cannot proceed forever. The growth of scallops reduces the number of channels among them. In turn this reduces the in-flux of Cu needed for the growth. In experiments, scallops of Cu_6Sn_5 were observed elongating in the growth direction after approximately 10 min of reaction at 200 °C. We analyze this transition behavior elsewhere; see Appendix B.

In the following section, we present first a simple model of growth of monosize scallops to illustrate the basic idea. Second, we present a general model illustrating the distributional growth of different sized scallops.

III. SIMPLE MODEL FOR MONOSIZE HEMISPHERES

Strictly speaking, the monosize distribution (size distribution as Dirac's function) is not compatible with scallop growth since scallop growth is parasitic and dependent upon the shrinkage of neighboring scallops. Therefore, the initial monosize distribution should be transformed into a wider-sized distribution. Yet all that is required is a narrow distribution function enabling us to ignore, for this specific model, the differences among the average values of the scallop radius, $\langle R\rangle, (\langle R^2\rangle)^{1/2}, (\langle R^3\rangle)^{1/3}, (\langle 1/R\rangle)^{-1}$, etc. The monosize approximation is good for a rough estimate of average values.

According to the first constraint that the interface between the scallops and Cu be occupied completely by scallops except the thin channels, we have

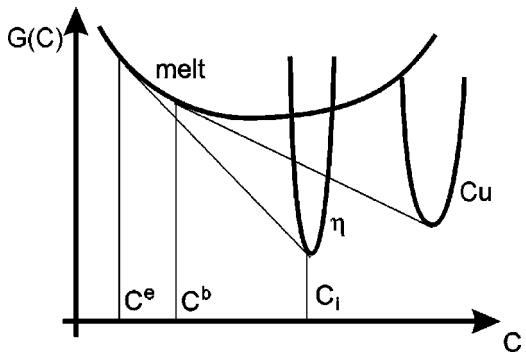

FIG. 2. Schematic dependence of the Gibbs free energy vs composition. The Cu quasiequilibrium concentration in the melt in the vicinity of the substrate (C^b), in the intermetallic compound Cu_6Sn_5 or η phase (C_i), and in the melt for stable equilibrium with planar η phase (C^e).

$$N\pi R^2 \cong S^{total} = \text{const}, \tag{3.1}$$

where N is the number of scallops. The free surface (the cross-sectional area of channels at the bottom) for the supply of Cu from the substrate is

$$S^{free} = N2\pi R\frac{\delta}{2} = \frac{\delta}{R}S^{total}, \tag{3.2}$$

where δ is the channel width. So the free surface decreases during the scallop growth as $1/R$. The volume of the reaction product of IMC scallops is equal to

$$V_i = N\frac{2\pi}{3}R^3 = \frac{2}{3}S^{total}R. \tag{3.3}$$

According to the second constraint that all influx of Cu atoms from the substrate be consumed by growing IMC scallops due to conservation of mass, we have

$$n_i C_i \frac{dV_i}{dt} = J^{in}S^{free}. \tag{3.4}$$

Here n_i is atomic density in IMC's, i.e., the number of atoms per unit volume, and C_i is atomic fraction of Cu in IMC's, which is 6/11 in Cu_6Sn_5. The influx is taken approximately as

$$J^{in} = -nD\frac{\left(C^e + \frac{\alpha}{R}\right) - C^b}{R}, \tag{3.5}$$

where n is the atomic density or number of atoms per unit volume in the melt or molten solder, $\alpha = C^e 2\gamma\Omega/R_G T$ in which γ is the isotropic surface tension at the IMC/melt interface, Ω is the molar volume, R_G is the gas constant, and T is the temperature. C^e is the equilibrium concentration (atomic fraction) of copper in solder at the planar interface between Cu_6Sn_5 and molten solder; C^b is equilibrium concentration of Cu in molten solder at the interface between substrate and solder at the channel's bottom (see Fig. 2). In our case $2\gamma\Omega/R_G T \approx 4.4\times 10^{-7}$ cm and $C^e \approx 0.003$.

First, we consider the case $\alpha/R << C^b - C^e$, so that

$$J^{in} \cong nD\frac{C^b - C^e}{R}. \tag{3.6}$$

Then, substituting Eqs. (3.6), (3.2), and (3.3) into the balance equation (3.4), we obtain

$$n_i C_i \frac{2}{3}S^{total}\frac{dR}{dt} = nD\frac{C^b - C_e}{R}\left(\frac{\delta}{R}S^{total}\right), \tag{3.7}$$

which immediately gives

$$R^3 = kt, \tag{3.8a}$$

$$k = \frac{9}{2}\frac{n}{n^i}\frac{D(C^b - C^e)\delta}{C_i}. \tag{3.8b}$$

Note that the surface tension is absent in the expression for the rate constant, despite the ''ripeninglike'' time law.

If we take $n/n_i \approx 1, C_i = \frac{6}{11}$, $D \approx 10^{-5}$ cm^2/s, $\delta \approx 5\times 10^{-6}$ cm, and $C^b - C^e \approx 0.001$, where the concentration C^b is taken for equilibrium of melt with the Cu_3Sn_1 phase, the rate constant $k \approx 4\times 10^{-13}$ cm^3/s. For example, for annealing time $t = 300$ s, it gives $R \approx 5\times 10^{-4}$ cm, which agrees very well with experimental data.[12,16]

Next, we consider what changes if we use the more correct expression in Eq. (3.5) for flux. In this case, the differential equation (3.7) for the $R(t)$ dependence changes to $3R^2 dR = k(1 - \alpha/R\Delta C)dt$, where $\Delta C = C^b - C^e$.

It can be integrated if we consider $\alpha/R\Delta C$ as a small parameter. Then,

$$kt \cong R^3 + \frac{3}{2}\frac{\alpha}{\Delta C}R^2. \tag{3.9}$$

The effective exponent for growth rate then is equal to

$$n^{ef} = \frac{d\ln R}{d\ln t} \cong \frac{1}{3}\left(1 + \frac{\alpha}{2R\Delta C}\right). \tag{3.10}$$

It demonstrates the deviation from the $t^{1/3}$ law. Yet these deviations are small for sizes exceeding 1 μm. For example, if we take $R = 10^{-4}$ cm and $\Delta C = 0.001$, we obtain $\alpha/2R\Delta C \approx 0.008$. Therefore, we will neglect the effect of the $\alpha/2R\Delta C$ term on the influx and will use Eq. (3.6) instead of Eq. (3.5).

According to the approximate equation (3.8) and relation (3.1), the number of scallops should depend on time as $t^{-2/3}$, as observed experimentally.[12,16] It seems astonishing that such a naive and simple model can fit the experimental data very well. The reason for this is an incoming flux being a rate-controlling step, determining the ripening rate during FDR.

We can understand now the crucial difference between the classical coarsening described by LSW theory and the flux-driven ripening described here. In the former the phase volume is almost constant at a sufficiently long time, and it is simply redistributed between grains. The driving force is a decrease of Gibbs free energy due to the decrease of total

surface of the phase. In our case the surface is constant (the total surface of hemispheres). Indeed,

$$S^{scallops/melt}=N2\pi R^2=2S^{total}=\text{const.} \tag{3.11}$$

Thus, in our case, the constant interfacial area is a constraint of the reaction. The driving force is the gain of Gibbs free energy from the increase of phase volume. This increase is possible owing to ''influx'' of Cu from the substrate. Therefore, we have flux-driven ripening in open systems. We should note that, of course, we are not the first to treat ripening in open systems. Slezov[3] treated ripening of voids by taking into account the vacancy flux moving towards the external boundaries in the theory of caking. Yet in that case there were no two-dimensional constraints, and the coarsening, even in nonhomogeneous conditions, proceeded due to a decrease of surface energy.

Evidently, the monosize model is oversimplified, since the growth of scallops cannot proceed without the shrinking of neighboring scallops. Thus, we should take the size distribution into account.

IV. BASIC EQUATIONS

Let $f(t,R)$ be the size distribution function, so that the total number of grains is equal to

$$N(t)=\int_0^\infty f(t,R)dR \tag{4.1}$$

and the average values are

$$\langle R^m\rangle=\frac{1}{N}\int_0^\infty R^m f(t,R)dR. \tag{4.2}$$

The first constraint of constant interface takes the form

$$\sum_{i=1}^{N}\pi R_i^2=\int_0^\infty \pi R^2 f(t,R)dR=S^{total}-S^{free}\cong S^{total}=\text{const.} \tag{4.3}$$

Surface area of channels for the copper supply is

$$S^{free}=\int_0^\infty \frac{\delta}{2}2\pi R f(t,R)dR. \tag{4.4}$$

The volume of the growing IMC scallops is

$$V_i=\sum_{i=1}^{N}\frac{2}{3}\pi R_i^3=\int_0^\infty \frac{2}{3}\pi R^3 f(t,R)dR. \tag{4.5}$$

The second major constraint on our open system is the conservation of mass; i.e., the ''influx'' is consumed by growing the IMC scallops,

$$n_i C_i\frac{dV_i}{dt}=J^{in}S^{free}. \tag{3.4'}$$

We shall take the influx density by analogy with the simplified model [Eq. (3.6)], replacing only the radius by its average value. Then

$$n_i C_i\frac{d}{dt}\int_0^\infty \frac{2}{3}\pi R^3 f(t,R)dR = nD\frac{\Delta C}{\dfrac{\int Rf(t,R)dR}{\int fdR}}\delta\int_0^\infty \pi R f(t,R)dR, \tag{4.6}$$

so that

$$\frac{\dfrac{d}{dt}\int_0^\infty R^3 f(t,R)dR}{\int_0^\infty f(t,R)dR}=\frac{\dfrac{d}{dt}\sum R_i^3}{N}=\frac{3\sum R_i^2\dfrac{dR_i}{dt}}{N}=\frac{3\displaystyle\int_0^\infty R^2\frac{dR}{dt}fdR}{N}=\frac{3}{2}\frac{n}{n_i}\delta\frac{D\Delta C}{C_i}. \tag{4.7}$$

Since scallops must grow and shrink atom by atom, the distribution function should satisfy the usual continuity equation in the size space:

$$\frac{\partial f}{\partial t}=-\frac{\partial}{\partial R}(fu_R), \tag{4.8}$$

where the velocity in the size space, u_R, is simply the growth rate of scallops with radius R, $u_R=dR/dt$, and is determined by the flux density on (or out of) each individual scallop:

$$\frac{dR}{dt}\cong\frac{-j(R)}{n_i C_i}. \tag{4.9}$$

In the transformations (4.7) and below, the derivative dN/dt is omitted since it should be multiplied by the cubed radius of disappearing scallops, which is naturally tending to zero.

In classic ripening theory, when each grain is spherical and is surrounded by infinite supersaturated solid solution, the expressions for $j(R)$ and dR/dt are found as a quasistationary solution of the diffusion problem in infinite space around a spherical grain with fixed supersaturation $\langle C\rangle - C^e$ at infinity:

$$u_R=\frac{dR}{dt}=\frac{n}{n_i}\frac{D}{C_i}\frac{\langle C\rangle-(C^e+\alpha/R)}{R}.$$

In our case the scallops almost touch each other (the situation being more close to the grain growth situation, but with the constraint of constant surface and increasing total volume). Therefore the classical expression is not applicable.

In FDR, the diffusional transport of copper atoms through the channels in the reaction zone is a rate-controlling step, since the ripening, which conserves the total surface area, would be impossible without growth and growth impossible without incoming flux. Under the constraint of constant surface, the rate of ripening will be controlled by the incoming flux, and this flux will be redistributed among scallops. (Of course, it does not mean that all scallops will grow—some of them will shrink.) When the incoming flux is zero, the ripening among the scallops changes to the classical case; i.e., the volume is conserved. Experimentally, this happens in the reaction between molten SnPb and a thin film of Cu when the film is consumed.[7].

Flux on (out of) each individual scallop should be proportional to the difference between the average chemical potential of copper μ in the reaction zone (we take it to be the same everywhere— a mean-field approximation) and the chemical potential at the curved scallop-melt interface, $\mu_\infty + \beta/R$, and $\beta = 2\gamma\Omega$:

$$-j(R) = L\left(\mu - \mu_\infty - \frac{\beta}{R}\right),$$

$$\frac{dR}{dt} = \frac{L}{n_i C_i}\left(\mu - \mu_\infty - \frac{\beta}{R}\right), \tag{4.10}$$

where the parameters L, μ are determined self-consistently from the above-mentioned two constraints—of constant surface and mass conservation. In Appendix C, we present the case when the flux on individual scallops is inversely proportional to its radius.

Indeed, the constant surface constraint implies

$$\begin{aligned}\frac{dS_{total}}{dt} &= 0\\ &= \frac{d}{dt}\sum 2\pi R_i^2\\ &= \sum 4\pi R_i \frac{dR_i}{dt}\\ &= \frac{4\pi L}{n_i C_i}\left((\mu - \mu_\infty)\sum R_i - \beta N\right),\end{aligned}$$

so that

$$\mu - \mu_\infty = \frac{\beta}{\langle R\rangle}. \tag{4.11}$$

The conservation law (4.7) implies

$$\begin{aligned}\frac{1}{2}\frac{n}{n_i}\delta\frac{D\Delta C}{C_i} &= \frac{\sum R_i^2 \frac{dR_i}{dt}}{N}\\ &= \frac{L}{n_i C_i N}\sum R_i^2\left(\frac{\beta}{\langle R\rangle} - \frac{\beta}{R_i}\right)\\ &= \frac{L\beta}{n_i C_i}\left(\frac{\sum R_i^2}{N\langle R\rangle} - \frac{\sum R_i}{N}\right)\\ &= \frac{L\beta}{n_i C_i}\frac{\langle R^2\rangle - \langle R\rangle^2}{\langle R\rangle},\end{aligned} \tag{4.12}$$

which immediately gives

$$L\beta = n_i C_i \frac{k}{9}\frac{\langle R\rangle}{\langle R^2\rangle - \langle R\rangle^2}, \tag{4.13}$$

so that

$$u_R = \frac{dR}{dt} = \frac{k}{9}\frac{1}{\langle R^2\rangle - \langle R\rangle^2}\left(1 - \frac{\langle R\rangle}{R}\right). \tag{4.14}$$

Thus in the mean-field approximation, the basic equation for the distribution function has the following form:

$$\frac{\partial f}{\partial t} = -\frac{k}{9}\frac{\langle R\rangle}{\langle R^2\rangle - \langle R\rangle^2}\frac{\partial}{\partial R}\left[f\left(\frac{1}{\langle R\rangle} - \frac{1}{R}\right)\right], \tag{4.15}$$

where the rate coefficient k is determined by the incoming flux conditions (first of all, by the channel width).

Equation (4.15) is the basic equation for distribution function in FDR theory. It contains the unknown parameter $\langle R\rangle$, which is equal to the critical radius, meaning only those scallops with R greater than $\langle R\rangle(t)$ can grow at the moment t.

V. SEMIANALYTICAL SOLUTION FOR THE MEAN-FIELD APPROXIMATION

We shall find the analytical solution of the basic equation (4.15). The structure of the basic equation hints that the following variables will be more convenient than t and R:

$$\tau = bt, \quad \xi = \frac{R}{(bt)^{1/3}} \tag{5.1}$$

(we will choose the most convenient value of b a bit later), so that

$$\frac{\partial}{\partial t} = b\left(\frac{\partial}{\partial \tau} - \frac{\xi}{3\tau}\frac{\partial}{\partial \xi}\right), \quad \frac{\partial}{\partial R} = \frac{1}{\tau^{1/3}}\frac{\partial}{\partial \xi}.$$

Then Eq. (4.15) takes the form

$$\tau\frac{\partial f}{\partial \tau} = \frac{\xi}{3}\frac{\partial f}{\partial \xi} - \frac{k}{9b}\frac{1}{\langle \xi^2\rangle - \langle \xi\rangle^2}\frac{\partial}{\partial \xi}\left[f\left(1 - \frac{\langle \xi\rangle}{\xi}\right)\right].$$

Let us choose

$$b=\frac{k}{9}\frac{1}{\langle\xi^2\rangle-\langle\xi\rangle^2}. \tag{5.2}$$

Then Eq. (5.3) transforms into

$$\tau\frac{\partial f}{\partial\tau}=\frac{\xi}{3}\frac{\partial f}{\partial\xi}-\frac{\partial}{\partial\xi}\left[f\left(1-\frac{\Xi}{\xi}\right)\right],\quad \Xi\equiv\langle\xi\rangle. \tag{5.3}$$

Furthermore, we look for a solution assuming that the parameter is constant (does not depend on time). In this case Eq. (5.3) suggests a separation of variables:

$$f(\tau,\xi)=g(\tau)\varphi(\xi). \tag{5.4}$$

Naturally, the validity of such a separation should be checked, after finding a solution, by substituting it in the constraints. Using Eq. (5.4), we transform Eq. (5.3) into

$$\frac{d\ln g}{d\ln\tau}=\frac{d\ln\varphi}{d\xi}\left(\frac{\xi}{3}-1+\frac{\Xi}{\xi}\right)-\frac{\Xi}{\xi^2}=\lambda=\text{const}. \tag{5.5}$$

The constant λ can be determined from the constraint of the invariable interface of scallop bottoms:

$$S^{total}=\pi\tau g(\tau)\int_0^\infty\xi^2\varphi(\xi)d\xi,$$

so that

$$g(\tau)=\frac{1}{\tau}\frac{S^{total}}{\pi\int_0^\infty\xi^2\varphi(\xi)d\xi}. \tag{5.6}$$

Therefore,

$$\ln g=-\ln\tau+\text{const},\quad \lambda=-1. \tag{5.7}$$

We will see below in Sec. VI that in the classical LSW conditions $\lambda=-4/3$. Using Eqs. (5.5) and (5.7), we obtain the following differential equation for the ''scaling part'' or ''time-independent part'' of the distribution function:

$$\frac{d\ln\varphi}{d\xi}=\frac{1}{\xi}+\frac{3-4\xi}{\xi^2-3\xi+3\Xi}. \tag{5.8}$$

Thus,

$$\varphi(\eta)=B_0\eta\exp\left\{\int_0^\eta\frac{3-4\xi}{\xi^2-3\xi+3\Xi}d\xi\right\},$$

$$\eta=\frac{R}{(bt)^{1/3}}. \tag{5.9}$$

The factor B_0 may be arbitrary since it will be cancelled in the product $g\varphi$. Hence, we will take it to be unity. Thus, the formal solution of our distribution function is

$$f(t,R)=\frac{B}{bt}\frac{R}{(bt)^{1/3}}\exp\left\{\int_0^{R/(bt)^{1/3}}\frac{3-4\xi}{\xi^2-3\xi+3\Xi}d\xi\right\}$$

$$=\frac{B}{\tau}\varphi(\eta),\quad \tau=bt,\eta=\frac{R}{(bt)^{1/3}}, \tag{5.10}$$

$$B=\frac{S^{total}}{\pi\int_0^\infty\xi^2\varphi(\xi)d\xi}. \tag{5.11}$$

The parameter is still unknown and should be determined from the condition of self-consistency:

$$\Xi=\langle\xi\rangle=\frac{\int\xi\varphi(\xi)d\xi}{\int\varphi(\xi)d\xi}. \tag{5.12}$$

The integral in Eqs. (5.9) or (5.10) strongly depends on the value of Ξ. The denominator $\xi^2-3\xi+3\Xi$ in the integral can have one real root, two real roots, or no real roots at all. We have three cases to be discussed in the following.

(A) If $\Xi>\Xi^*\equiv3/4$, then denominator has no real roots.

(B) For $\Xi=\Xi^*\equiv3/4$, we have two equal positive roots

$$\xi_1=\xi_2=3/2. \tag{5.13a}$$

(C) For $\Xi<\Xi^*\equiv3/4$, we have two different positive roots

$$\xi_1=\frac{3}{2}+\sqrt{\frac{9}{4}-3\Xi},\quad \xi_2=\frac{3}{2}-\sqrt{\frac{9}{4}-3\Xi}. \tag{5.13b}$$

In case (A), the integral in Eq. (5.9) never diverges; it has no singularities for $\xi>0$. Then the standard integration procedure gives (Ref. 21; see pp. 82–84)

$$\varphi(\eta)=\text{const}\times\frac{\eta}{\left[\left(\eta-\frac{3}{2}\right)^2+3\langle\eta\rangle-\frac{9}{4}\right]^2}$$

$$\times\exp\left[-\frac{3}{\sqrt{3\langle\eta\rangle-\frac{9}{4}}}\arctan\frac{\eta-\frac{3}{2}}{\sqrt{3\langle\eta\rangle-\frac{9}{4}}}\right]. \tag{5.14}$$

In case (B) a standard integration gives

$$\varphi(\eta)=0,\quad \eta>\left(\frac{3}{2}\right),$$

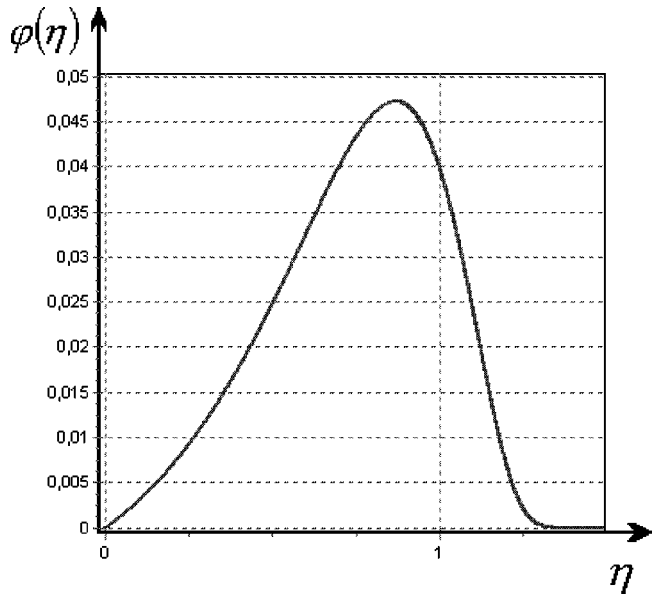

FIG. 3. Scaling part $\varphi(\eta)$, $\eta=R/(bt)^{1/3}$ of the size distribution $f(t,R)=g(\tau)\varphi(\eta)$ in the FDR model for case (B) ($\Xi=\Xi^*=<\xi>=3/4$), for which a self-consistency condition is satisfied: $\int_0^\infty \eta\varphi(\eta,\Xi)d\eta/\int_0^\infty \varphi(\eta,\Xi)d\eta=\Xi$.

$$\varphi(\eta)=\text{const}\times\frac{\eta}{\left(\frac{3}{2}-\eta\right)^4}\exp\left(-\frac{3}{\frac{3}{2}-\eta}\right),\quad 0<\eta<\left(\frac{3}{2}\right) \tag{5.15}$$

(see Fig. 3).

In case (C), the indefinite integral shows two singularities at positive roots $\xi_1>\xi_2>0$. It should mean that nondimensional grain size should not exceed the lessen of these two positive roots (ξ_2): $R<\xi_2(bt)^{1/3}$. Thus, an explicit form of the scaling part of distribution function is the following:

$$\varphi(\eta)=0 \text{ if } \eta>\xi_2,$$

$$\varphi(\eta)=\text{const}\times\eta(\xi_2-\eta)^{(4\xi_2-3)/(\xi_1-\xi_2)}\times(\xi_1-\eta)^{(3-4\xi_1)/(\xi_1-\xi_2)} \text{ if } \eta<\xi_2. \tag{5.16}$$

In order to find out what kind of distribution function should be observed, we should use a self-consistency condition (5.12). This relation can be considered as the transcendent equation for determining the parameter Ξ, which in turn determines the shape of function $\varphi(\eta)$. The dependence of the expression $\int_0^\infty \eta\varphi(\eta,\Xi)d\eta/\Xi\int_0^\infty \varphi(\eta,\Xi)d\eta$ on parameter Ξ is easily obtained by numerical integration and is demonstrated at Fig. 4. We can see that this expression is equal to unity only for regime (B) ($\Xi=3/4$); for other values, it is always less than unity. Thus, regime (B) gives us a unique asymptotical solution. For this case

$$\langle\xi^2\rangle-\langle\xi\rangle^2=0.0615,\ \langle\xi\rangle=3/4=\xi_{\max}/2,\ \langle\xi^3\rangle=0.5535.$$

Then the parameter

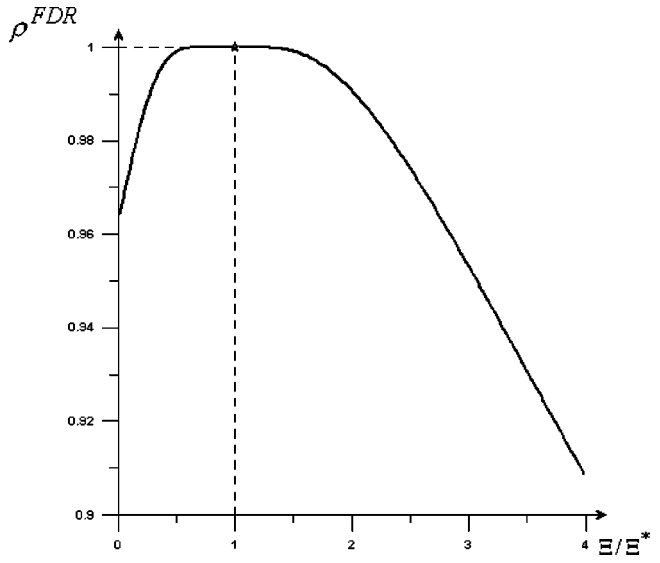

FIG. 4. Dependence of the ratio $\int_0^\infty \eta\varphi(\eta,\Xi)d\eta/\Xi\int_0^\infty \varphi(\eta,\Xi)d\eta$ on parameter Ξ/Ξ^* for the FDR case ($\Xi^*=3/4$). This ratio is equal to unity (self-consistency condition) only for regime (B): $\Xi/\Xi^*=1$.

$$b=\frac{k}{9\times 0.0615}=\frac{k}{0.5535}. \tag{5.17}$$

Hence, average cube of grain size is equal to

$$\langle R^3\rangle=\langle\xi^3\rangle bt=kt, \tag{5.18}$$

which coincides with the result of the monosize model, but for the averaged cube.

The averaged size will be

$$\langle R\rangle=\langle\xi\rangle(bt)^{1/3}=\frac{3}{4}\left(\frac{k}{0.5535}t\right)^{1/3}=0.913(kt)^{1/3}. \tag{5.19}$$

Thus, the asymptotical size distribution during FDR satisfies the universal scaling expression (5.15), different from the LSW case. The rate of ripening and growth is determined by the incoming flux conditions.

VI. ALTERNATIVE DERIVATION OF THE LSW ASYMPTOTIC SOLUTION

For a direct comparison, it is interesting to apply the above approach to the case of classical coarsening in a three-dimensional closed system (LSW case). We present an alternative derivation of the LSW distribution function and solutions below. The equation for the size distribution function is well known:

$$\frac{\partial f}{\partial t}=-a_0\frac{\partial}{\partial R}\left[\frac{f}{R}\left(\langle C\rangle-C^e-\frac{\alpha}{R}\right)\right],\quad a_0=\frac{n}{n_i}\frac{D}{C_i}. \tag{6.1}$$

For the late stage of coarsening, the mass conservation equation is

$$n_iC_iV_i+n\langle C\rangle(V-V_i)=nC_0V, \tag{6.2}$$

$$V_i=\int_0^\infty \frac{4}{3}\pi R^3 f(t,R)dR \ll V, \quad \langle C\rangle \to C^e, \tag{6.3}$$

and n_i, C_i, and V_i are, respectively, the atomic density, atomic fraction, and volume of the new phase undergoing coarsening in the matrix phase of n, $\langle C\rangle$(initially C_0,) and $V-V_i$ (initially V), respectively. The constraint of the constant new phase volume is

$$V_i=\int_0^\infty \frac{4}{3}\pi R^3 f(t,R)dR \cong \frac{n(C_0-C^e)}{n_i C_i}V=\text{const.} \tag{6.4}$$

Equation (6.4) is the only constraint on the LSW size distribution function since the system is closed. In other words,

$$\frac{d}{dt}\int_0^\infty R^3 f dR = 0 = -a_0\int_0^\infty R^3 \frac{\partial}{\partial R}\left[\frac{f}{R}\left(\langle C\rangle - C^e - \frac{\alpha}{R}\right)\right]dR. \tag{6.5}$$

Using the zero boundary conditions for $f(R)$, we obtain the supersaturation as

$$\Delta \equiv \langle C\rangle - C^e = \alpha\frac{\int f dR}{\int R f dR}=\frac{\alpha}{\langle R\rangle}, \tag{6.6}$$

which means that in the LSW case the critical radius is simply an average one.

The condition of Eq. (6.6) transforms Eq. (6.1) into

$$\frac{\partial f}{\partial t}=-A\frac{\partial}{\partial R}\left[\frac{f}{R}\left(\frac{1}{\langle R\rangle}-\frac{1}{R}\right)\right], \quad A=\frac{n}{n_i}\frac{D\alpha}{C_i}. \tag{6.7}$$

Using new variables $\tau=At, \xi=R/(At)^{1/3}$ and solving for a solution with separation of variables, $f=\tilde{g}(\tau)\tilde{\varphi}(\xi)$, we obtain

$$\frac{d\ln\tilde{g}}{d\ln\tau}=\frac{d\ln\tilde{\varphi}}{d\xi}\left(\frac{\xi}{3}-\frac{1}{\langle\xi\rangle}\frac{1}{\xi}+\frac{1}{\xi^2}\right)-\left(\frac{2}{\xi^3}-\frac{1}{\langle\xi\rangle}\frac{1}{\xi^2}\right)=\lambda = \text{const.} \tag{6.8}$$

To find the parameter λ, we should use the constraint of constant volume (instead of constant surface in the FDR case):

$$\tilde{g}(\tau)\frac{4\pi}{3}\tau^{4/3}\int \xi^3\tilde{\varphi}(\xi)d\xi=\frac{n}{n_i}\frac{\Delta_0}{C_i}V, \tag{6.9}$$

which means that

$$\tilde{g}(\tau)=\text{const}\times\tau^{-4/3}, \quad \lambda=-\frac{4}{3}. \tag{6.10}$$

Using Eq. (6.10) in Eq. (6.8), we obtain

$$\frac{d\ln\tilde{\varphi}}{d\xi}=\frac{2}{\xi}+3\frac{1/\langle\xi\rangle-2\xi^2}{\xi^3-3\xi/\langle\xi\rangle+3}. \tag{6.11}$$

Thus,

$$\tilde{\varphi}(\eta)=\eta^2\exp\left\{\int_0^\eta \frac{3\tilde{\Xi}-6\xi^2}{\xi^3-3\tilde{\Xi}\xi+3}d\xi\right\}, \quad \tilde{\Xi}\equiv\frac{1}{\langle\xi\rangle}. \tag{6.12}$$

The formal solution for the LSW distribution function is

$$f(t,R)=\frac{B_{LSW}}{(At)^{4/3}}\frac{R^2}{(At)^{2/3}}\exp\left\{\int_0^{R/(At)^{1/3}}\frac{3\tilde{\Xi}-6\xi^2}{\xi^3-3\tilde{\Xi}\xi+3}d\xi\right\}$$

$$=\frac{B_{LSW}}{\tau^{4/3}}\tilde{\varphi}(\eta),$$

$$\tau=At, \eta=\frac{R}{(At)^{1/3}}, \quad B_{LSW}=\frac{\frac{n}{n_i}\frac{\Delta_0}{C_i}V}{\frac{4}{3}\pi\int_0^\infty \xi^3\tilde{\varphi}(\xi)d\xi}. \tag{6.13}$$

The parameter $\tilde{\Xi}$ should be found from the following condition:

$$\frac{1}{\tilde{\Xi}}=\langle\xi\rangle=\frac{\int_0^\infty \xi\tilde{\varphi}(\xi,\tilde{\Xi})d\xi}{\int_0^\infty\tilde{\varphi}(\xi,\tilde{\Xi})d\xi}. \tag{6.14}$$

To solve this equation, we need to know the explicit form of the function. As in the FDR case, we have three possibilities and three corresponding explicit forms found by standard integration.

(A) $\tilde{\Xi}<\tilde{\Xi}^*\equiv(3/2)^{2/3}$, single, negative root:

$$\xi_1=-\sqrt{\tilde{\Xi}^*}\{[1+\sqrt{1-(\tilde{\Xi}/\tilde{\Xi}^*)^3}]^{1/3}+[1-\sqrt{1-(\tilde{\Xi}/\tilde{\Xi}^*)^3}]^{1/3}\},$$

$$\varphi(\eta)=\eta^2\left(1+\frac{\eta}{|\xi_1|}\right)^{(3\tilde{\Xi}-6\xi_1^2)/2\xi_1^2+3/|\xi_1|)}\left(\frac{3/|\xi_1|}{\eta^2+\xi_1\eta+3/|\xi_1|}\right)^{(6\xi_1^2+18/|\xi_1|+3\tilde{\Xi})/[2(2\xi_1^2+3/|\xi_1|)]}$$

$$\exp\left\{\frac{3|\xi_1|\left(3/|\xi_1|-\xi_1^2+\frac{3}{2}\tilde{\Xi}\right)}{(3/|\xi_1|+2\xi_1^2)\sqrt{3/|\xi_1|-\xi_1^2/4}}\left[\arctan\frac{\eta-|\xi_1|/2}{\sqrt{3/|\xi_1|-\xi_1^2/4}}+\arctan\frac{|\xi_1|/2}{\sqrt{3/|\xi_1|-\xi_1^2/4}}\right]\right\}. \tag{6.15}$$

(B) $\tilde{\Xi}=\tilde{\Xi}^*\equiv(3/2)^{2/3}$ ($\xi_1=\xi_2=\sqrt{\tilde{\Xi}^*}$, $\xi_3=-2\sqrt{\tilde{\Xi}^*}$): $\varphi(\eta)=0, \eta>(\frac{3}{2})^{1/3}$,

$$\varphi(\eta)=\frac{\eta^2 e^1 \exp\left(-\dfrac{1}{1-\eta/\sqrt{\tilde{\Xi}^*}}\right)}{\left(1+\dfrac{\eta}{2\sqrt{\tilde{\Xi}^*}}\right)^{7/3}\left(1-\dfrac{\eta}{\sqrt{\tilde{\Xi}^*}}\right)^{11/3}}, \quad \eta<\left(\frac{3}{2}\right)^{1/3}. \tag{6.16}$$

(C) For $\tilde{\Xi}>\tilde{\Xi}^*\equiv(3/2)^{2/3}$, we have two different positive and one negative root: $\xi_1=2\sqrt{\tilde{\Xi}}\cos(\phi/3)$, $\xi_2=-2\sqrt{\tilde{\Xi}}\cos(\phi/3+\pi/3)$, $\xi_3=-2\sqrt{\tilde{\Xi}}\cos(\phi/3-\pi/3)$, $\cos(\phi)=-3/2\tilde{\Xi}^{3/2}$ ($\xi_1>\xi_2>0$, $\xi_3<0$); $\varphi(\eta)=0, \eta>\xi_2$;

$$\varphi(\eta)=\eta^2\left(1-\frac{\eta}{\xi_1}\right)^{(3\tilde{\Xi}-6\xi_1^2)/[(\xi_1-\xi_2)(\xi_1-\xi_3)]}\left(1-\frac{\eta}{\xi_2}\right)^{(3\tilde{\Xi}-6\xi_2^2)/[(\xi_2-\xi_3)(\xi_2-\xi_1)]}\left(1+\frac{\eta}{|\xi_3|}\right)^{(3\tilde{\Xi}-6\xi_3^2)/[(\xi_3-\xi_1)(\xi_3-\xi_2)]}, \quad \eta<\xi_2. \tag{6.17}$$

Substituting expressions (6.15)–(6.17) into Eq. (6.14) for a wide region of $\tilde{\Xi}$ values, we can check [by numerical calculation of integrals in Eq. (6.14)] that this equation is satisfied strictly for $\tilde{\Xi}=\tilde{\Xi}^*\equiv(9/4)^{1/3}$. For all other values the product $\tilde{\Xi}\int\xi\tilde{\varphi}(\xi,\tilde{\Xi})d\xi/\int\tilde{\varphi}(\xi,\tilde{\Xi})d\xi$ is less than unity.

It means that only regime (B), with $\langle\xi\rangle=1/\tilde{\Xi}^*=(\frac{2}{3})^{2/3}$ and the distribution, given by Eq. (6.16), is self-consistent. Thus, the critical size changes with time as

$$R_{cr}=\langle R\rangle=\langle\xi\rangle At^{1/3}=\left(\frac{4}{9}\frac{n}{n_i}\frac{D\alpha}{C_i}t\right)^{1/3},$$

which is the same as the classical LSW result. The size distribution function presented in Eq. (6.16) is the same as the asymptotic LSW expression.

Thus, the method developed here for FDR can be applied to the LSW case as well. It serves as a check of its validity. However, the shortcoming of this method is the use of numeric integration (though very simple). Nevertheless, its positive feature as demonstrated by the alternative derivation of LSW results is that only two approximations are used—constant volume and separation of variables.

VII. DISCUSSION

The results of previous sections can be discussed briefly as follows.

(i) In Sec. III, under the assumption of an approximately monosize distribution, the growth of the average scallop size satisfies the $t^{1/3}$ law, with the growth constant being practically independent of surface tension. It does not mean that ripening does not proceed during growth. On the contrary, the growth is parasitic due to the constraint of a constant bottom interface and close proximity of hemispherical scallops. It means that in this case the ripening is driven not by a decrease of surface energy (it remains constant) but by a gain of bulk free energy due to the chemical reaction to form IMC's.

(ii) In Secs. IV and V, when we take the size distribution into account but remain in the framework of the ''mean-field approximation'' (neglecting the difference of the melt composition in different places of the reaction zone), the rate of the size distribution widening [Eqs. (5.10), (5.15), and (5.17)] appears to depend on the incoming flux. More precisely, it appears to depend on the product of the melt diffusivity, channel width, and difference of equilibrium compositions between the melt with IMC's and the melt with the substrate [Eq. (3.8b)]. The lesser is this product, the slower is the size distribution widening and average size growth. Concerning the parameters in the product, we note that the channel width is not precisely known so far. It may have a width distribution depending on the orientation relationship of the two neighboring scallops. But as can be seen in Fig. 1(c), it can exceed substantially the width of a large-angle grain boundary. Another parameter of concern is the difference of equilibrium concentrations. If the melt is in contact with pure copper (in the early stage of the reaction), this concentration difference is about 3.7 at %. Then, if the melt is in contact with Cu_3Sn_1 (at the later stage), the difference is about 0.1 at %.

(iii) We would like to point out that the proposed analysis for flux-driven ripening is far from being complete. We have treated scallops as preserving their hemispherical shape during the flux-driven ripening. As we know from experiments, it is not true for long annealing (reflow) time—say, over 1 h at 200 °C for eutectic SnPb on Cu; the scallops will become elongated. The hemispherical shape in our model is interrelated with the mean-field approximation. If we take into account the different compositions of melt at different distances from the substrate, the growth rate in different places of the same scallop will be different—and the shape will change. We intend to study such a ''gradient'' model in the near future.

(iv) In Sec. VI, when the proposed method is applied to the classical coarsening case, it gives results in good agreement with the LSW theory. Using the same method to analyze the LSW ripening and flux-driven ripening, we conduct

TABLE I. Comparison of physical differences between LSW and FDR models.

LSW	FDR
Closed system	Open system
Constant volume, decreasing surface	Constant surface, increasing volume
Driving force, reduction of surface energy	Driving force, gain of bulk free energy
One constraint (constant volume)	Two constraints (constant surface area, volume growth rate proportional to influx)
Number of grains decreasing as t^{-1}	Number of grains decreasing as $t^{-2/3}$
$\langle R\rangle^3=k^{LSW}t$, the rate constant $k^{LSW}$is proportional to surface tension $k^{LSW}=\frac{4}{9}\frac{n}{n_i}\frac{D\alpha}{C_i}$	$\langle R^3\rangle=kt$, the rate constant k is independent of surface tension, $\langle R\rangle^3=(0.913)^3kt, k=\frac{9}{2}\frac{n}{n_i}\frac{D(C^b-C^e)\delta}{C_i}$

a direct comparison of them in Tables I and II.

(v) For a detailed check of FDR theory, an accurate determination of the size distribution is needed. Both cross-section images and plain-view images are required. From the plain-view images, the distribution function $f(S)$ of scallops on the bottom surface can be determined, which can be converted into the size distribution according to $f(R)=f(S)dS/dR=2\sqrt{\pi S}f(S)$.

(vi) We believe that the general idea of a flux-driven redistribution of sizes in open systems has wider applications rather than merely the FDR. For example, it may apply to flux-driven grain growth and flux-driven precipitation.

VIII. CONCLUSION

We have presented a theory of three-dimensional growth and ripening in open systems with two-dimensional (2D) constraint of the constant surface. In this case the ripening is driven not by a decrease of surface energy but by a gain of bulk free energy due to a chemical reaction. The growth kinetics and size distribution have been predicted. The size distribution is controlled by the condition of incoming flux. The theory gives a reasonable kinetic description of scallop-type intermetallic compound formation during the reaction between molten solder and solid copper.

TABLE II. Comparison of mathematical differences between LSW and FDR models.

LSW	FDR
$\int R^3 f(R)dR\cong\text{const}$	$\int R^2 f(R)dR\cong\text{const}$
$-j(R)=nD\frac{\langle C\rangle-C^e-\frac{\alpha}{R}}{R},\quad \alpha=\frac{2\gamma\Omega}{R_GT}C^e,$	$-j(R)=L\left(\mu-\mu_\infty-\frac{\beta}{R}\right),\beta=2\gamma\Omega$
$\frac{dR}{dt}=A\left[\frac{1}{R}\left(\frac{1}{\langle R\rangle}-\frac{1}{R}\right)\right],\quad A=\frac{n}{n_i}\frac{D\alpha}{C_i}$	$\frac{dR}{dt}=\frac{k}{9}\frac{\langle R\rangle}{\langle R^2\rangle-\langle R\rangle^2}\left(\frac{1}{\langle R\rangle}-\frac{1}{R}\right),$ $k=\frac{9}{2}\frac{n}{n_i}\frac{D(C^b-C^e)\delta}{C_i}$
$\frac{\partial f}{\partial t}=-A\frac{\partial}{\partial R}\left[\frac{f}{R}\left(\frac{1}{\langle R\rangle}-\frac{1}{R}\right)\right],\quad A=\frac{n}{n_i}\frac{D\alpha}{C_i}$	$\frac{\partial f}{\partial t}=-\frac{k}{9}\frac{1}{\langle R^2\rangle-\langle R\rangle^2}\frac{\partial}{\partial R}\left[f\left(1-\frac{\langle R\rangle}{R}\right)\right]$
Formal solution (our form)	Formal solution
$f(t,R)=\frac{B_{LSW}}{(At)^{4/3}}\frac{R^2}{(At)^{2/3}}\exp\left\{\int_0^{R/(At)^{1/3}}\frac{3\tilde{\Xi}-6\xi^2}{\xi^3-3\tilde{\Xi}\xi+3}d\xi\right\}$	$f(t,R)=\frac{B}{bt}\frac{R}{(bt)^{1/3}}\exp\left\{\int_0^{R/(bt)^{1/3}}\frac{3-4\xi}{\xi^3-3\xi+3\Xi}d\xi\right\}=\frac{B}{\tau}\varphi(\eta)$
Explicit solution	Explicit solution
$\varphi(\eta)=\frac{\eta^2e^1\exp\left(-\frac{1}{1-\eta/\sqrt{\Xi^*}}\right)}{\left(1+\frac{\eta}{2\sqrt{\Xi^*}}\right)^{7/3}\left(1-\frac{\eta}{\sqrt{\Xi^*}}\right)^{11/3}},$	$\varphi(\eta)=\frac{\eta}{(\frac{3}{2}-\eta)^4}\exp\left(-\frac{3}{\frac{3}{2}-\eta}\right),$
$\eta<(\frac{3}{2})^{1/3}$	$0<\eta<3/2$
$\eta=R/(At)^{1/3}$	$\eta=R/(bt)^{1/3},\quad b=\frac{k}{0.5535}$

ACKNOWLEDGMENTS

The authors would like to thank for support National Science Foundation Contract No. DMR-9987484 and Semiconductor Research Corporation Contract No. NJ-774. They also would like to thank V. V. Slezov (Kharkov Institute of Physics and Technology) for a critical review of the manuscript and A. Ardell (UCLA) for helpful comments. Figure 1(b) was taken by T. Y. Lee and J. W. Suh (UCLA). Figure 1(c) was taken by George T. T. Sheng (MXIC, Taiwan, ROC).

APPENDIX A: ASSUMPTIONS ABOUT INFLUX AND OUTFLUX OF CU IN THE REACTION ZONE

We assume that the influx of Cu supplied by the interfacial diffusion of Cu from the bottom of scallops to the channels (or/and Sn diffusion in opposite direction) is not a limiting step of the scallop growth. When all Cu atoms in the influx are taken from the bottom of the scallops and supplied by the interfacial diffusion along the interface between the Cu and scallops, conservation of mass implies

$$J^{lateral} 2\pi R \delta^{\mathrm{int}} \cong J^{in} 2\pi R \frac{\delta}{2}. \tag{A1}$$

Here δ is the channel width, δ^{int} is the width of the interfacial boundary between scallops and Cu (its width about 0.5 nm), $J^{lateral}$ and J^{in} are the flux densities of Cu, respectively, along the interface and along the channel into the melt. We can estimate the influx density (per unit area) as

$$J^{in} \cong nD \frac{C^b - C^e}{R}, \tag{A2}$$

where n is the atomic density of molten solder, D is the Cu diffusivity in molten solder, C^b is the equilibrium concentration of Cu in molten solder, contacting directly with Cu (without IMC in between), C^e is the equilibrium concentration of Cu in molten solder, contacting with IMC's along the flat interface, and R is the average size of hemispherical scallops taken here as an estimate for the dimension of the reaction (diffusion) zone.

To estimate the flux along the interface substrate/grain bottom, we will use a quasistationary approximation for the diffusion at the interface. Let

$$J(r) = -n_{\mathrm{int}} D^{\mathrm{int}} \frac{dC}{dr} 2\pi r \delta^{\mathrm{int}} \tag{A3}$$

be the lateral flux at distance r from the center. Further we will neglect (for a rough estimation) the differences between the atomic density in different phases and at the interface (n_{int}). Due to the consumption of copper by the growing IMC's, the substrate's surface moves in opposite direction to influx ["down" in Fig. 1(a)] with a velocity U_S. The interfacial layer between each scallop and the substrate moves with the same velocity in the same direction (otherwise the interface would become "curved"). In this direction every thin slice of area $2\pi r dr$ obtains per unit time an additional number of copper atoms, $n(1-C_i)2\pi r dr U_S$. Then conservation of matter in quasistationary conditions implies

$$J(r) + n(1-C_i)2\pi r dr U_S = J(r+dr). \tag{A4}$$

This simple differential equation gives us

$$J(r) = \pi n (1-C_i) U_S r^2. \tag{A5}$$

Substituting Eq. (A5) into Eq. (A.3), we obtain one more simple differential equation for the concentration, which after integration gives

$$\int_{C(0)}^{C(R)} D^{\mathrm{int}} dC = (1-C_i)\frac{R^2}{4\delta^{\mathrm{int}}} U_S, \tag{A6}$$

where

$$U_S \approx \frac{\delta}{R} D \frac{C^b - C^e}{R}. \tag{A7}$$

We note that the difference of upper and lower limits of the integral cannot exceed the homogeneity range ΔC.

The left-hand side of Eq. (A.6) in the limiting case $C(R)-C(0)=\Delta C$ is often called an integrated Wagner diffusivity $D^{\mathrm{int}}\Delta C$.[22,23] Since an IMC has a narrow homogeneity composition range, it is more convenient to express the integrated diffusivity in terms of the chemical potential μ or Gibbs free energy per atom, g, and a self-diffusivity D^* of Cu in the interface (we neglect the Sn self-diffusivity):

$$\begin{aligned}\int_{\Delta C} D^{\mathrm{int}} dC &\cong \int_{\Delta C} [(1-C)D^* + 0] \frac{C(1-C)}{k_B T} \frac{d^2 g}{dC^2} dC \\ &\cong D^* \frac{C_i (1-C_i)^2}{k_B T} \left(\frac{g_{i+1} - g_i}{C_{i+1} - C_i} + \frac{g_{melt} - g_i}{C_i - C^e} \right) \\ &> (1-C_i)\frac{R^2}{4\delta^{\mathrm{int}}} U_S. \end{aligned} \tag{A8}$$

Here C_{i+1} and g_{i+1} are respectively, the copper atomic fraction and Gibbs free energy per atom for the substrate (Cu or Cu_3Sn).

From Eqs. (A7) and (A8) we obtain a condition for diffusivity at the interface not to be the rate-limiting step of FDR: Its explicit form depends on whether we consider the substrate phase as Cu or Cu_3Sn. If the substrate is copper, then

$$\begin{aligned} D^* &> \frac{\delta (C^b - C^e)}{4 C_i (1-C_i) \delta^{\mathrm{int}}} \frac{k_B T}{\left(\frac{g_{Cu} - g_i}{1-C_i} + \frac{g_{melt} - g_i}{C_i - C^e} \right)} D \\ &= \frac{\delta (C^b - C^e)}{4\delta^{\mathrm{int}}} \frac{R_G T}{(-\Delta g_\eta^f)} D, \end{aligned} \tag{A9a}$$

where the formation energy of the η phase[24]

$$\Delta g_\eta^f = (-7139.4 + 0.315\,92T) \ \mathrm{J/mol}, \quad C^b - C^e \cong 0.037.$$

If the substrate is $Cu_3Sn(\varepsilon)$, then

$$D^* > \frac{\delta(C^b - C^e)}{4C_i(1-C_i)\delta^{\text{int}}} \frac{k_B T}{\left(\frac{g_\epsilon - g_i}{C_\epsilon - C_i} + \frac{g_{melt} - g_i}{C_i - C^e}\right)} D. \tag{A9b}$$

Using the formation energy of the ε phase, $\Delta g^f = (-8479.6 + 0.318\,36T)$ J/mol,[24] we obtain for the copper self-diffusivity at the interface $D^* > 10^{-7}$ cm^2/s, which is a rather restrictive condition. It may be that it is a reason why sometimes a wavy interface between scallops and substrate is observed (higher in the center of a scallop and lower at the channel positions).

Concerning outflux, we have assumed that it is negligible. It is related to the assumption that all Cu atoms, dissolved in molten solder, feed the growing IMC scallops. If the amount of molten solder is small, it will become saturated with Cu very quickly, and the saturation time $t = H^2/D$ is about 10 s for a solder bump with a diameter of $H = 0.01$ cm. In this case our assumption is good. On the other hand, if the molten solder is unlimited, the problem is complicated. The balance equation can be modified in the following way:

$$n_i C_i \frac{dV_i}{dt} = J^{in} S^{free} - J^{out} S^{total}. \tag{A10}$$

Here V_i is the volume of growing IMC's, S^{free} is the area of channels between scallops at the bottom, and S^{total} is the total area of substrate. The outflux can be estimated according to standard expression

$$J^{out} = nC^e \left(\frac{D}{\pi t}\right)^{1/2} \exp\left(-\frac{R^2}{4Dt}\right), \tag{A11}$$

where we take R as a characteristic dimension of the reaction zone. For real experimental data ($D \approx 10^{-5}$ cm^2/s, R = several micrometers, $t = 5$–15 min) the ratio $R^2/4Dt$ is very small, so the exponent is almost unity. S^{free} can be estimated as $(\delta/R)S^{total}$.

For the assumption of negligible outflux to be valid, it is necessary that

$$J^{out} S^{total} \ll J^{in} S^{free}. \tag{A12}$$

The left-hand side (total outflux) decreases with $t^{-1/2}$ dependence. The right-hand side decreases inversely proportional to the squared scallop size, which (according to experimental data and our analysis) grows by a $t^{1/3}$ law. Thus, the total influx decreases with time by the $t^{-2/3}$ law, which is faster than outflux, due to ripening and the respective decrease of the channel total length. Therefore, at some moment the outflux can approximately equalize the influx. In this case the growth of IMC's can substantially slow down—it will be suppressed by the diffusion into a nonsaturated melt. The condition in Eq. (A12) can be easily transformed to

$$R^2 \ll \frac{C^b - C^e}{C^e} (\pi D t)^{1/2} \delta. \tag{A13}$$

As we have given in Sec. III,

$$R = (kt)^{1/3}, \quad \text{where } k = \frac{9}{2}\frac{n}{n_i} D \frac{C^b - C^e}{C_i}\delta. \tag{A14}$$

Substituting Eq. (A14) into Eq. (A13), we obtain the condition for neglecting the outflux:

$$t \ll \left(\frac{C^b - C^e}{C^e}\right)^2 \left(\frac{2n_i}{9n}\right)^4 \left(\frac{C_i}{C^e}\right)^4 \pi^3 \frac{\delta^2}{D} \tag{A15a}$$

or, in other terms,

$$R \ll \left(\frac{2\pi n_i}{9n}\right) \frac{C_i(C^b - C^e)}{(C^e)^2}\delta. \tag{A15b}$$

For $C^b - C^e = 10^{-3}$, $C^e = 3 \times 10^{-3}$, and $\delta = 5 \times 10^{-6}$ cm, Eq. (A15b) gives $R \ll 2 \times 10^{-4}$ cm, $t \ll 20$ s, which is too restrictive for FDR applications. Yet, by varying the parameters, we can obtain reasonable numbers.

Thus, for a molten solder saturated with copper (for which experiments are usually made), the FDR should apply and it has predicted the average sizes, which coincide with experimental data. For an unsaturated melt, the FDR model may not apply or be marginal. The above condition gives unreasonably small times, after which the FDR should be suppressed. Thus, we can conclude that the saturation of a melt or negligible outflux is a necessary condition for the observation of FDR.

APPENDIX B: TRANSITION FROM HEMISPHERICAL SCALLOPS TO ELONGATED SCALLOPS

Elongated scallops are observed at the later stages of the reaction, when ripening practically stops. At least one of the general reasons for this is presented below. As we show here the rate of Gibbs free energy release, which is proportional to the rate of volume change, depends on time as $t^{-2/3}$ in FDR. For a columnar growth it depends on time as $t^{-1/2}$ (if we neglect any 2D ripening among the columns). It is evident that since the time dependence on "$-2/3$" is sharper than "$-1/2$," at some moment FDR growth will become less favorable than columnar growth. A detailed analysis will be given elsewhere.

APPENDIX C: ALTERNATIVE SCHEME OF FDR FOR THE CASE WHEN THE FLUX ON INDIVIDUAL GRAIN IS INVERSELY PROPORTIONAL TO ITS RADIUS.

We derived the size distribution of scallops during FDR for the case when the flux of copper on an individual grain is proportional to the difference of the average chemical potential in the reaction zone and the chemical potential in the vicinity of the curved scallop/melt interface. Here we will present a theory for the case when the liquid solution has enough space to form a quasistationary copper distribution around each hemispherical grain, so that instead of Eq. (4.10) we have

$$-j(R)=\frac{\tilde{L}}{R}\left(\mu-\mu_\infty-\frac{\beta}{R}\right),\quad \frac{dR}{dt}=\frac{1}{n_iC_i}\frac{\tilde{L}}{R}\left(\mu-\mu_\infty-\frac{\beta}{R}\right), \tag{C1}$$

where the parameters L,μ are determined self-consistently from the above-mentioned two constraints of constant surface and mass conservation.

Indeed, the constant surface constraint implies

$$\begin{aligned}\frac{dS_{total}}{dt}&=0\\&=\frac{d}{dt}\sum 2\pi R_i^2\\&=\sum 4\pi R_i\frac{dR_i}{dt}\\&=\frac{4\pi\tilde{L}}{n_iC_i}\left((\mu-\mu_\infty)N-\beta\sum\frac{1}{R_i}\right),\end{aligned}$$

so that

$$\mu-\mu_\infty=\beta\left\langle\frac{1}{R}\right\rangle. \tag{C2}$$

The mass conservation constraint implies

$$\begin{aligned}\frac{1}{2}\frac{n}{n_i}\delta\frac{D\Delta C}{C_i}&=\frac{\sum R_i^2\frac{dR_i}{dt}}{N}\\&=\frac{\tilde{L}\beta}{n_iC_i}\left(\left\langle\frac{1}{R}\right\rangle\langle R\rangle-1\right),\end{aligned} \tag{C3}$$

which immediately gives

$$\tilde{L}\beta=n_iC_i\frac{k}{9}\frac{1}{\left\langle\frac{1}{R}\right\rangle\langle R\rangle-1}, \tag{C4}$$

so that

$$u_R=\frac{dR}{dt}=\frac{k}{9}\frac{1}{\left\langle\frac{1}{R}\right\rangle\langle R\rangle-1}\frac{1}{R}\left(\left\langle\frac{1}{R}\right\rangle-\frac{1}{R}\right). \tag{C5}$$

Then, in the mean-field approximation, the basic equation for the distribution function has the following form:

$$\frac{\partial f}{\partial t}=-\frac{k}{9}\frac{1}{\left\langle\frac{1}{R}\right\rangle\langle R\rangle-1}\frac{\partial}{\partial R}\left[\frac{f}{R}\left(\left\langle\frac{1}{R}\right\rangle-\frac{1}{R}\right)\right], \tag{C6}$$

where the rate coefficient k is determined by the incoming flux conditions.

Equation (C6) is the basic equation for the distribution function in our alternative scheme of FDR theory. It contains the unknown parameter $\langle 1/R\rangle$, which is equal to the inverse critical radius, meaning only those scallops with $R>[\langle 1/R\rangle\times(t)]^{-1}$ can grow at the moment t.

To find an asymptotical solution of the basic equation (C6), we use the following variables: $\tau=bt$, $\xi=R/(bt)^{1/3}$,

$$b=\frac{k}{9}\frac{1}{\left\langle\frac{1}{\xi}\right\rangle\langle\xi\rangle-1}. \tag{C7}$$

Then Eq. (C7) transforms into

$$\tau\frac{\partial f}{\partial\tau}=\frac{\xi}{3}\frac{\partial f}{\partial\xi}-\frac{\partial}{\partial\xi}\left[\frac{f}{\xi}\left(\hat{\Xi}-\frac{1}{\xi}\right)\right],\quad \hat{\Xi}\equiv\left\langle\frac{1}{\xi}\right\rangle. \tag{C8}$$

Furthermore, we look for a solution assuming a separation of variables:

$$f(\tau,\xi)=g(\tau)\varphi(\xi). \tag{C9}$$

$$\frac{d\ln g}{d\ln\tau}=\frac{d\ln\varphi}{d\xi}\left(\frac{\xi}{3}-\hat{\Xi}\frac{1}{\xi}+\frac{1}{\xi^2}\right)-\left(\frac{2}{\xi^3}-\hat{\Xi}\frac{1}{\xi^2}\right)=\lambda=\text{const}. \tag{C10}$$

The constant can be determined from the constraint of the invariable interface of scallop bottoms:

$$g(\tau)=\frac{1}{\tau}\frac{S^{total}}{\pi\int_0^\infty\xi^2\varphi(\xi)d\xi}. \tag{C11}$$

Therefore,

$$\ln g=-\ln\tau+\text{const},\quad \lambda=-1. \tag{C12}$$

Then in full analogy with Secs V and VI, one obtains the formal solution

$$\begin{aligned}f(t,R)&=\frac{B}{bt}\frac{R^2}{(bt)^{2/3}}\exp\left\{\int_0^{R/(bt)^{1/3}}\frac{3\hat{\Xi}-5\xi^2}{\xi^3-3\hat{\Xi}\xi+3}d\xi\right\}\\&=\frac{B}{\tau}\varphi(\eta),\quad \tau=bt,\quad \eta=\frac{R}{(bt)^{1/3}},\end{aligned} \tag{C13}$$

$$B=\frac{S^{total}}{\pi\int_0^\infty\xi^2\varphi(\xi)d\xi}. \tag{C14}$$

The parameter $\hat{\Xi}$ is still unknown and should be determined from the condition of self-consistency:

$$\hat{\Xi}=\left\langle\frac{1}{\eta}\right\rangle=\frac{\int\frac{1}{\eta}\varphi d\eta}{\int\varphi d\eta}. \tag{C15}$$

We have three cases

(A) For $\hat{\Xi}<\hat{\Xi}^*\equiv(3/2)^{2/3}$, the denominator has a single, negative root.

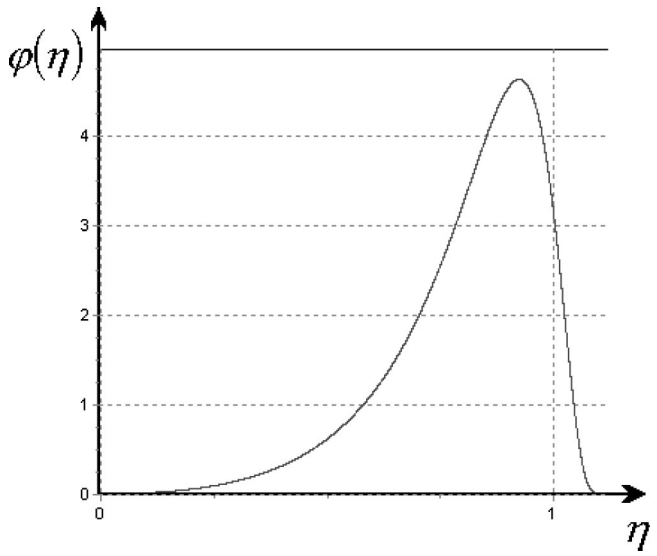

FIG. 5. Scaling part $\varphi(\eta), \eta = \frac{R}{(bt)^{1/3}}$ of size distribution $f(t,R)=g(\tau)\varphi(\eta)$ in the alternative scheme of FDR model for case B ($\hat{\Xi}=\hat{\Xi}^*=<\xi>^{-1}=(3/2)^{2/3}$), for which a self-consistency condition is satisfied.

(B) For $\hat{\Xi}=\hat{\Xi}^*\equiv(3/2)^{2/3}$, we have one negative and two equal positive roots.

(C) For $\hat{\Xi}>\hat{\Xi}^*\equiv(3/2)^{2/3}$, we have two different positive and one negative root.

Calculations, similar to those of Sec. VI, show that only one value $\hat{\Xi}=\hat{\Xi}^*\equiv(3/2)^{2/3}$ satisfies a self-consistency condition and provides the following distribution, more similar to LSW, but with different exponents:

$$\varphi(\eta)=0, \quad \eta>\left(\frac{3}{2}\right)^{1/3},$$

$$\varphi(\eta)=\frac{\eta^2 e^{2/3}\exp\left(-\dfrac{2/3}{1-\eta/\sqrt{\hat{\Xi}^*}}\right)}{\left(1+\dfrac{\eta}{2\sqrt{\hat{\Xi}^*}}\right)^{17/9}\left(1-\dfrac{\eta}{\sqrt{\hat{\Xi}^*}}\right)^{28/9}}, \quad \eta<\left(\frac{3}{2}\right)^{1/3}. \tag{C16}$$

The plot of $\varphi(\eta)$ against η is shown in Fig. 5.

Thus, regime (B) gives us a unique asymptotical solution. For this case

$$\left\langle\frac{1}{\xi}\right\rangle\langle\xi\rangle-1\cong 0.0665, \langle\xi\rangle=0.814, \langle\xi^3\rangle\cong 0.6.$$

The ratio of mean-squared deviation and mean size is about 0.20. Then, the parameter $b=k/(9\times 0.0665)=k/0.6$. Hence, the average cube of grain size is equal to

$$\langle R^3\rangle=\langle\xi^3\rangle bt=kt,$$

which coincides with the result of the monosize model, but for the averaged cube. The averaged size will be

$$\langle R\rangle=\langle\xi\rangle(bt)^{1/3}\cong 0.814\left(\frac{k}{0.6}t\right)^{1/3}.$$

Thus, again, as in Sec. IV, the ripening rate is determined by the influx condition, but the size distribution is different, with r^2 behavior for small sizes. Also it is different from the LSW distribution due to the constraint of constant surface area.

*On leave from Department of Theoretical Physics, Cherkasy State University, Ukraine.

[1] I.M. Lifshiz and V.V. Slezov, J. Phys. Chem. Solids **19**, 35 (1961).
[2] C. Wagner, Z. Electrochem, Z. Elektrochem. **65**, 581 (1961).
[3] V.V. Slezov, *Theory of Diffusion Decomposition of Solid Solution* (Harwood Academic, Dordrecht, 1995).
[4] D. Frear, D. Gravas, and J.W. Morris, Jr., J. Electron. Mater. **16**, 181 (1986).
[5] P.A. Vianco, P.E. Hlava, and A.C. Kilgo, J. Electron. Mater. **23**, 583 (1993).
[6] H.K. Kim, H.K. Liou, and K.N. Tu, Appl. Phys. Lett. **66**, 2337 (1995).
[7] Ann A. Liu, H.K. Kim, K.N. Tu, and P.A. Totta, J. Appl. Phys. **80**, 2774 (1996).
[8] P.S. Teo, Y.W. Huang, C.H. Tung, M.R. Marks, and T.B. Lim, *Proceedings of IEEE 1995 Electronic Component and Technology Conference* (IEEE, Piscataway, NJ, 2000), p. 33.
[9] K.H. Prakash and T. Sritharan, Acta Mater. **49**, 2481 (2001).
[10] R.S. Rai, S.K. Kang, and S. Purushothaman, *Proceedings of IEEE 1995 Electronic Component and Technology Conference* (IEEE, Piscataway, NJ, 1995), p. 1197.
[11] S. Chad, W. Laub, J.M. Sabee, and R.A. Fournelle, J. Electron. Mater. **28**, 1194 (1996).
[12] H.K. Kim and K.N. Tu, Phys. Rev. B **53**, 16 027 (1996).
[13] D.R. Frear, J.W. Kang, J.K. Lin, and C. Zhang, JOM **53**, 28 (2001)
[14] F. Barteks, J.W. Morris, Jr., G. Dalke, and W. Gust, J. Electron. Mater. **23**, 787 (1994).
[15] S. Bader, W. Gust, and H. Hieber, Acta Metall. Mater. **43**, 329 (1995).
[16] R.A. Gagliano and M.E. Fine, JOM **53-6**, 33 (2001).
[17] Pascal Oberndorff, Ph.D. thesis, Technical University of Eindhoven, Eindhoven, The Nerthelands, 2001.
[18] K.N. Tu and K. Zeng, Mater. Sci. Eng., R. **34**, 1 (2001).
[19] K.N. Tu, Fiona Ku, and T.Y. Lee, J. Electron. Mater. **30**, 1129 (2001).
[20] J.H. Lee, J.H. Park, Y.H. Lee, Y.S. Kim, and D.H. Shin, J. Mater. Res. **16**, 1227 (2001).
[21] I.S. Gradshteyn and I.M. Ryzhik, *Table of Integrals, Series and Products*, 5th ed. (Academic Press, New York, 1993).
[22] F.J.J. van Loo, Prog. Solid State Chem. **20**, 47 (1990).
[23] A.M. Gusak, and M.V. Yarmolenko, J. Appl. Phys. **73**, 4881 (1993).
[24] W.J. Boettinger, C.A. Handwerker, and U.R. Kattner, in *The Mechanics of Solder Alloy Wetting and Spreading*, edited by by F.G. Yost, F.M. Hosking, and D.R. Frear (Van Nostrand, Reinhold, New York, 1993) p. 103.